Journal Pre-proof

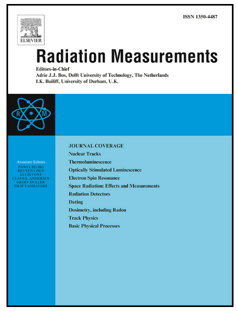

Thoron exhalation rate measurement – findings from a large worldwide intercomparison study

G. de With, G. Venoso, A. Maiorana, C. Di Carlo, O. Meisenberg, Q. Guo, M. Janik, E.D. Nugraha, O.M. Bobbo, C. Kranrod, M. Hosoda, S. Tokonami, B.K. Sahoo, S.D. Kanse, J. Tschiersch

PII: S1350-4487(25)00100-3

DOI: https://doi.org/10.1016/j.radmeas.2025.107471

Reference: RM 107471

To appear in: *Radiation Measurements*

Received Date: 14 March 2025

Revised Date: 11 May 2025

Accepted Date: 30 May 2025

Thoron exhalation rate measurement – findings from a large worldwide intercomparison study

G. de With[1,*], G. Venoso[2], A. Maiorana[2], C. Di Carlo[2], O. Meisenberg[3], Q. Guo[4], M. Janik[5], E. D Nugraha[6]*, O. M. Bobbo[6], C. Kranrod[7], M. Hosoda[6,7], S. Tokonami[7], B.K. Sahoo[8], S.D. Kanse[8] and J. Tschiersch[9]**

[1] NRG PALLAS, Utrechtseweg 310, NL-6800 ES Arnhem, The Netherlands.

[2] Istituto Superiore di Sanità (Italian National Institute of Health), Centro Nazionale per la Protezione dalle Radiazioni e Fisica Computazionale (National Center for Radiation Protection and Computational Physics), Viale Regina Elena, 299, 00161 Roma, Italy.

[3] Private person, München, Germany.

[4] Peking University, State Key Laboratory of Nuclear Physics and Technology, 100871 Beijing, China.

[5] National Institutes for Quantum Science and Technology (QST), National Institute of Radiological Sciences (NIRS), Department of Radiation Measurement and Dose Assessment, Radiation Measurement Group, 4-9-1 Anagawa, Inage-ku, 263-8555 Chiba, Japan.

[6] Hirosaki University Graduate School of Health Sciences, Department of Radiation Science, 66-1 Hon-cho, Hirosaki 036-8564, Japan.

[7] Hirosaki University, Institute of Radiation Emergency Medicine, 66-1 Hon-cho, Hirosaki 036-8564, Japan.

[8] Radiological Physics and Advisory Division Bhabha Atomic Research Center, CTCRS Building, Anushaktinagar, Mumbai-400 094, India.

[9] Helmholtz Zentrum München GmbH, former Institute of Radiation Protection, Ingolstädter Landstr. 1, 85764 Neuherberg, Germany.

* Present address: Research Center for Safety, Metrology, and Nuclear Technology, The National Research and Innovation Agency of Indonesia (BRIN), Tangerang Selatan, Banten, Indonesia
** Present address: Institute of Geological and Mining Research, P.O. Box 4110, Yaoundé, Cameroon

Conflicts of Interest statement

Authors declared no conflict of interest.

[*] Corresponding author. NRG Arnhem, Utrechtseweg 310, P.O. Box 9034, 6800 ES Arnhem, The Netherlands.
E-mail address: G.deWith@nrg.eu (G. de With).

ABSTRACT

A global intercomparison study was conducted to measure the thoron (^{220}Rn) exhalation rate from two building materials, with participation from five European laboratories and three Asian laboratories. The test samples—phosphogypsum and unfired clay—were circulated among the laboratories using a sequential proficiency testing scheme. The assigned values and their uncertainties were determined through recommended robustness analysis. For comparison, the classical method, which uses the arithmetic mean of all participants' results, was also applied. Individual measurement results were evaluated for bias, precision, and proficiency in accordance with ISO 13528:2022.

The assigned exhalation rates were (0.39 ± 0.15) Bq m^{-2} s^{-1} for phosphogypsum and (0.53 ± 0.15) Bq m^{-2} s^{-1} for unfired clay. Z-scores were below 3 for seven of the nine methods used. Bias (R_b) and precision (P) parameters were within 50%, except in one case. Laboratories provided details on Type A and Type B uncertainties, revealing that detector calibration uncertainty was the dominant factor in most cases.

These findings underscore the need for more robust calibration methods to improve the accuracy of thoron measurements. The development of a harmonized standard would greatly enhance the consistency of thoron exhalation rate measurements. Such a standard should provide guidance on detector calibration, as well as key factors such as climate conditions during sample preparation and testing, procedures for determining exhalation rates and their uncertainties, and considerations for material aging and spatial variations.

KEYWORDS: natural radioactivity, ^{220}Rn, exhalation rate, building materials, interlaboratory comparison

1 INTRODUCTION

1.1 Background

The presence of the radioactive gas radon (^{222}Rn) in the indoor environment is well known and is one of the major sources of radioactive exposure for general members of the public. Risk assessments for radon both in mines and in residential settings have provided clear insights into the health risks due to radon. As a result, radon is now recognized as the second most important cause of lung cancer after smoking in the general population. Consequently, exposure to radon in dwellings and workplaces is subject of regulatory control. Health risks are, however, predominantly associated with the radon isotope ^{222}Rn located in the decay series of the primordial radionuclide ^{238}U. Nevertheless, exposure to the shorter-lived isotope ^{220}Rn (Thoron) from the primordial radionuclide ^{232}Th can also be significant. According to UNSCEAR (2016) thoron is responsible for around 10-20% of the combined radiation dose from the radon isotopes in dwellings. However, this contribution can vary considerably, as it is dependent on local soil composition and the choice of building materials.

A limited number of surveys on thoron (progeny) concentrations in dwellings and workplaces were carried out. Measurement of indoor thoron concentrations were, for example, recently performed by Sanada (2021) and Chen (2022). Nation-wide surveys measuring thoron progeny concentration are scarce. Among them, the most extensive survey was carried out in the Netherlands and completed in 2015, and included around 2500 dwellings (Smetsers et al., 2018). The survey showed an average thoron progeny concentration (Equilibrium Equivalent Thoron Concentration, EETC) of around 0.65 Bq m^{-3} with a median value of 0.53 Bq m^{-3} and a maximum of 13 Bq m^{-3}. In 2017, a follow-up survey was carried out in workplaces with comparable findings. The study by De With et al. (2018) also quantified the contribution of different types of building materials. Based on the dose coefficients reported in UNSCEAR (2006) and 80% time spent indoors, this results in a mean dose of about 0.18 mSv per year. For the measured maximum EETC value, the dose was estimated to be more than 2 mSv. A recent study by Hu et al. (2022) reported average EETC values of approximately 1 $Bq \cdot m^{-3}$ in the Chinese regions Beijing and Changchun, and the Japanese region Aomori. Earlier studies performed in thoron prone areas, e.g. in China (Wang et al.,1996, Shang et al., 2008) and India (Sreenath Reddy et al., 2004), demonstrated that thoron exposure can be well in excess of 4 mSv per year based on 80% indoor time (Meisenberg and Tschiersch, 2010). Moreover, in modern homes with reduced ventilation (e.g. for energy saving reasons) even higher indoor inhalation doses are possible according to Meisenberg et al. (2017).

1.2 Thoron and building materials

The dominant source of thoron in residential housing are the mineral based building materials, and particularly those with a high content of ^{228}Ra and ^{228}Th from the ^{232}Th decay series. The half-life of thoron is 55s and considerably smaller than radon with a half-life of 3.8 days. As a consequence, the ability of thoron to migrate through porous media such as soil and building materials is significantly less than that of radon. A physical parameter that characterizes migration of thoron through the porous media is the diffusion length, typically denoted as L. It reflects the average distance thoron atoms travel by diffusion before undergoing radioactive decay. The diffusion length L is defined as $L = \sqrt{\frac{D}{\lambda}}$ where D is the diffusion coefficient of the thoron gas in the material ($m^2\ s^{-1}$) and λ (s^{-1}) is the nuclear decay constant of thoron. It is important to note that the diffusion coefficient is an element specific parameter that is the same for radon and thoron. A typical diffusion length for thoron is around 0.1 and up to 1 cm in respectively concrete and gypsum, while the diffusion length for radon is approximately two orders of magnitude higher.

Therefore, building materials that can be prone to thoron exhalation are bulk materials such as concrete and finishing or surface materials such as gypsum and unfired clay. The material features that play a key role in the exhalation of thoron from the building material are: the ^{224}Ra concentration (thoron's direct mother nuclide), thoron emanation fraction, the material's microstructure (e.g. porosity and water content). These features determine (i.) the production of thoron, (ii.) migration from the material grain, and (iii.) transport through the building material.

Once thoron is present in the indoor environment, the highest concentrations are found near the source (building material). Consequently, thoron concentrations in the environment are not uniform, which is in strong contrast with the longer lived ^{222}Rn. A detailed description on the mechanisms and complexities involved in the transport and formation of thoron and its progenies in dwellings is described by De With and De Jong (2011; 2016).

Systematic measurement of the thoron exhalation rate from building materials is limited. In the early 80's the thoron exhalation rate from some building materials were measured by Keller et al. (1982) and Folkerts et al. (1984). In recent years, some studies were dedicated to the measurement of the thoron exhalation rate from building materials e.g. De With et al. (2014), and more recently by Čeliković et al. (2020). Frutos-Puerto et al. (2020) measured the thoron exhalation from some building materials used on the Iberian Peninsula, such as cement, different granites, slate and gypsum. Nguyên et al. (2021) investigated the thoron exhalation from unfired mud, which is used as building material for earthen dwellings, and found exhalation rates as high as 3.5 Bq m^{-2} s^{-1}. They also constructed a mud house typical for the region and measured indoor thoron concentrations. An overview of the thoron exhalation rate for some of the mainstream building materials is presented in Table 1.

1.3 Quality standards and intercomparison studies

Initiatives to improve the quality of thoron exhalation measurements, such as interlaboratory comparisons and harmonised measurement protocols are very scarce. Measurement protocols used by the laboratories are mostly based on in-house procedures built on individual expertise. An international harmonised standard from ISO or CEN is presently not available. The authors are only aware of a single interlaboratory comparison on thoron exhalation from building materials that was published in 2021 by De With et al. (2021). However, this intercomparison was limited to five laboratories and indicated considerable variation in measurement results. In addition, the analysis did not follow the latest statistical methods for use in proficiency testing as described in ISO 13528 (2022). Therefore, a 2nd interlaboratory comparison on thoron exhalation from building materials was launched, and its findings are reported in this paper. A total of eight laboratories have participated in the study, each of the laboratories using their own measurement procedure and testing conditions.

This paper provides a description of the tested materials and the test procedures used by the individual laboratories followed by a summary and discussion of the test results. The paper is completed by a short list of recommendations to improve robustness of the determination methods.

2 MATERIALS AND METHODS

2.1 Samples

Two samples, which represent realistic building materials with increased thoron exhalation, were prepared for the intercomparison. Sample I was prepared by NRG (Netherlands) and made from phosphogypsum. Its surface was 11 cm × 11 cm, and its thickness was 2 cm. Sample II was provided by the Helmholtz institute (Germany) and consisted of a baseplate of fibreboard (not contributing to the thoron exhalation), 1 cm of clay base plaster and 1 cm of clay finish plaster mixed from kaolinite and sand 0-2 mm and was produced by a professional clay plasterer. Its size was also 11 cm × 11 cm. The specific activities of natural radionuclides in the two samples were determined by gamma spectroscopy of the raw materials and are presented in Table 2. The mixing ratio of the raw materials for sample II is unknown but represents a suitable mixing ratio for the production of clay plaster. Both samples were sealed on all sides except the front face (sample I with plastic tape, sample II with lacquer) in order to ensure a realistic exhalation from a single surface and to avoid boundary effects at the edges of the samples. It was checked that thoron could not diffuse through the sealing with other samples that were sealed at all surfaces.

The interlaboratory comparison was conducted using the sequential scheme of proficiency testing (para 3.2 of ISO 13528:2022), i.e. the same samples were distributed sequentially to all partners for measurement. In contrast with the simultaneous scheme, for which different samples are distributed to the partners, the sequential scheme requires much more time to be completed and, as the number of participants increases, so does the time. Nevertheless, the sequential scheme approach currently represents the most feasible option for this kind of measurements. In fact, due to the extremely small diffusion length in building materials, most of the thoron emitted from a surface originates from a very thin outer layer of approximately a few mm's (de With et al., 2021; Porstendörfer, 1994). Given that the thoron exhalation is highly dependent on surface roughness and imperfections of the materials, it is challenging to produce copies of the same building material sample with reduced variability.

2.2 Experimental methods

A total of nine test methods were applied in this study, operated by: the Nuclear Research and consultancy Group (The Netherlands), Helmholtz Zentrum München (Germany), Meisenberg (private person, Germany), Peking University (China), National Institutes for Quantum Science and Technology (Japan), Hirosaki University (Japan), Bhabha Atomic Research Center (India) and the Italian National Institute of Health (Italy).

All applied methods experimentally determine the thoron concentration in an exhalation chamber, often called as accumulation chamber, where the sample is located. This accumulation chamber is complemented with a thoron detector. A typical schematic of the test method used by the laboratories is shown in Figure 1. The chamber provides a controlled environment with known temperature and humidity conditions, known geometrical features and ventilation conditions, to enable calculation of the exhalation rate E_{Tn} according to the following equation:

$$E_{Tn} = \frac{C_{Tn} \cdot V \cdot \lambda_{eff}}{S}, \quad (1)$$

where E_{Tn} is the thoron exhalation rate (Bq m^{-2} s^{-1}); S is the surface area (m^2), which is 0.11×0.11 m^2; C_{Tn} is the average thoron activity concentration in the chamber (Bq m^{-3}); λ_{eff} is the effective decay constant (s^{-1}); V is the free volume (m^3); λ_{Tn} is the thoron decay constant (s^{-1}) and λ_v is the ventilation exchange rate (s^{-1}). In case no ventilation is applied λ_v=0, otherwise the ventilation exchange rate is defined as $\lambda_v=\phi/V$, where ϕ is the air or nitrogen flow in m^3 s^{-1}. Back-diffusion into the sample is neglected because of the short half-life of the nuclide.

Contrary to radon, the thoron concentration reaches steady state within a few minutes due to its short half-life. For this reason, all test methods can start measurement shortly after the sample is put in place. Furthermore, thoron concentration is fairly independent of the ventilation rates with values of 0.5 h^{-1} or lower. Nevertheless, the presence of radon poses a specific challenge in the determination of the thoron exhalation rate and requires discrimination between ^{220}Rn and ^{222}Rn. Moreover, since thoron concentrations would normally be expected to be high in the vicinity of the sample and decrease with distance, all detection methods use artificial air mixing.

Five institutions have used an electrostatic collection type radon and thoron monitor (RAD7, DURRIDGE, USA). In this device, thoron and radon decay products in the air are deposited by electrostatic precipitation onto a silicon alpha detector with subsequent spectrometer. Three other institutions used the following radon/thoron monitors: SMART RnDuo, the Tracelab ERS-2-S and the RTM2200 from SARAD to measure thoron gas concentration. All these instruments employ spectrometry to discriminate between radon and thoron. By analysing the decays of thoron daughters on the detector, the thoron concentration in air is calculated using specific calibration factors. Finally, one institution also performed a measurement with a passive detection technique based on CR-39 (a solid-state nuclear track detector). This technique offers several advantages over active methods, such as cost-effective, simple to deploy, and therefore ideal for large-scale surveys. However, these methods traditionally face several challenges, including radon/thoron discrimination, higher measurement uncertainty, lack of real-time data capabilities, and longer processing times due to chemical etching and track reading procedures. To address these limitations, particularly the crucial issue of radon/thoron discrimination, researchers have developed several innovative approaches. The twin-cup method (Tokonami et. al., 2005; Sahoo et. al., 2013) has emerged as a leading solution. This technique employs a diffusion barrier that exploits the significant difference in diffusion lengths and half-lives between ^{222}Rn and ^{220}Rn, and is used in this study.

Further details that are specific for each of the methods are described below and a listing of the key features is provided in Table 3.

2.2.1 Lab A

The test setup is based on the test arrangement used for measuring the radon exhalation rate from building materials. This arrangement and the required test procedures are described in the

Dutch standard NEN 5699 (NEN, 2001). For the determination of the thoron exhalation rate, the exhalation chamber is equipped with fans to ensure uniform mixing of the thoron. For accurate climate control the exhalation chamber with a volume of around 30 L is equipped with temperature control and purged with a nitrogen flow of 300 mL min^{-1} and 50% relative humidity. The temperature in the exhalation chamber is set to 20 ^{o}C and the measurement time is by default set to 24 h to enable good statistics. The conditioning of the samples prior to measurement was continued until the decrease in moisture content of the material was less than 0.07% measured over a period of 7 days (NEN, 2001). A full description of the calibration procedure as well as the measurement characteristics of the test facility such as linearity, repeatability and presence of a uniform thoron concentration are reported by De With et al. (2014).

2.2.2 Lab B

Dry air is conveyed with a volume flow rate of about 1 L min^{-1} in the device. The device was calibrated at Physikalisch-Technische Bundesanstalt (PTB Braunschweig, Germany); the calibration is traceable (Röttger et al., 2010). For the exhalation rate measurement, the device is connected in closed circuit to an air-tight chamber of about 3 L volume containing the sample (Tuccimei et al., 2006). All samples are placed in the chamber for at least one day prior to the measurement in order to adjust the moisture content of the samples to the humidity of the chamber. Sample moisture saturation is assumed when a stable humidity in the chamber is achieved. Standard moisture conditions are important as exhalation depends on the humidity of the sample (Tschiersch and Meisenberg, 2008). The induced turbulence of the air flow of the measurement loop provides a well-mixed atmosphere inside the small chamber.

2.2.3 Lab C

The test setup used a 3 L accumulation chamber combined with a semiconductor type detector (TracerLab ERS-2-S) for measuring both radon and thoron. It was attached to the chamber in pumping mode in a closed loop so that mixing of the air inside the chamber was provided. The device was calibrated at the Physikalisch-Technische Bundesanstalt (PTB, Braunschweig, Germany) with traceability to a national standard. Where needed the device was purged with clean air prior to any measurement. Prior to the measurement the sample was kept at those conditions for several days. The humidity inside the accumulation chamber was controlled by using a saturated solution of potassium carbonate (saturation humidity 44%). The measurement device was calibrated for the ambient thoron concentration, and the exhalation rate was determined according to Eq. (1). Each sample was measured three times using a measurement time of 2 h for each determination. An additional correction factor was applied in order to take into account the decay of thoron during its progress through the closed loop from the inlet of the measurement device to its outlet (Kanse et al., 2013).

2.2.4 Lab D

The sample was enclosed in an air-tight chamber of about 3 L. A sensor was put inside the chamber to record temperature and humidity. The chamber was connected to a Nafion membrane dryer and the RAD7. Instead of the RAD7 accessory desiccant, the Nafion membrane (PD-50T-12MSS, Perma Pure LLC) was applied as the dryer. This Nafion membrane dryer can let the water molecular penetrate through from the moist side to the dry side, while the thoron atom cannot penetrate through the membrane. By this way, the moisture is removed from the air sample. Samples of building material were tested with and without thoron seal. For thoron seal, only one side of the sample is kept bared to provide thoron exhalation while other sides are wrapped by aluminium foil. Each sample was measured for at least 24 hours. The thoron exhalation rate is calculated according to Eq. (1), and the C_T need to be modified according to the RAD7 manual considering the thoron decay during the gas circuit.

2.2.5 Lab E

The RAD7 is connected to the chamber in a closed-loop pumping mode to ensure mixing of the air in the accumulation chamber. The details for methodology have been published in the previous literature (Hosoda et al., 2022). The RAD7 has been calibrated in a radon/thoron exposure chamber, with traceability to the PTB, Germany (Pornnumpa et al., 2018). The instrument was purged with clean air prior to each measurement. In addition, the temperature and relative humidity inside and outside the accumulation chamber were monitored using portable type meteorological monitors (TR-73U, T&D Corporation, Japan). The mass of the samples was reduced by 0.1 g before and after the measurements. Each sample is measured 5 times with a measurement time of 5 h for each determination at a flow rate of 1 L min^{-1}. An additional correction factor is applied to take account of the decay of thoron as it passes through the closed loop from the inlet to the outlet of the measuring device. The thoron exhalation rate was calculated using Eq (1) where the ventilation rate is assumed zero (see. 2.2.2).

2.2.6 Lab F

The test setup consists of a 6.75 L accumulation chamber and a semiconductor type detector radon and thoron monitor (RTM2200, Sarad Gmbh, Germany). The monitor was calibrated by the manufacturer and checked using a calibration rock source provided by DURRIDGE Inc, USA. The system was a closed loop in which the gas was circulated continuously with the flow rate (0.3 lpm) generated by an internal pump. The measurement cycle was set as 4 hours and measurements were conducted repeatedly for 28 h in each sample. Saturated salt/water solution was used to maintain stable relative humidity inside the exhalation chamber. To maintain homogeneous thoron distribution within the chamber, a small fan was installed. The chamber tightness was checked by an appropriate test utilizing N_2 gas.

In addition to the active method, the thoron exhalation rate was also measured using a passive method within the same type of accumulation chamber. Solid-state nuclear track detectors (SSNTDs) commercially known as BARYOTRAK (Fukuvi Chemical Industry, Japan), mounted within a RADUET-type monitor were employed to determine thoron (and radon) concentrations (Yasuda et al., 1999, Tokonami et al., 2005). After exposure CR-39 chips were chemically etched in 6.25 M NaOH solution for 18 hours at 70 ^{o}C. Finally, the counting system for reading and analysis described elsewhere was applied (Kodaira et al., 2016). The detectors were calibrated in the QST radon and thoron calibration chambers, as detailed by Tokonami et al. (2005).

2.2.7 Lab G

The thoron exhalation rate was measured using a closed-loop experimental setup that comprised an accumulation chamber (1.2 L) and a ZnS:Ag-based SMART RnDuo detector (AQTEK System, India). The small volume of the accumulation chamber, along with a fan attached internally to the chamber's top surface, ensured uniform mixing of thoron gas within the chamber. This uniform mixing is essential to prevent underestimation and ensure accurate measurements when using the accumulation technique. The detector's internal pump, with a flow rate of 0.75 L min^{-1}, drew samples from the accumulation chamber into the detector for measurement and then re-circulated the gas back into the chamber. The detector was calibrated against standard radon/thoron concentrations generated in a calibration chamber using a Pylon TH1025 thoron source. To ensure the accuracy of the measurements, the performance of the instrument is routinely compared with other detectors, such as the AlphaGUARD (Saphymo GmbH, Germany) and RAD7. The measurements were unaffected by changes in environmental parameters like humidity. Measurements were conducted with thoron exhaling from one face of the cuboidal sample block, using a measurement cycle of 1 hour, over a duration of 1 day. The thoron exhalation rate was calculated using Eq (1), with a correction factor, β, incorporated to account for re-circulation of thoron gas and the dilution of its concentration inside the detector and tubing (Kanse et al., 2013; Kanse et al., 2020). The β value for this setup was estimated to be 1.15.

2.2.8 Lab H

The sample has been placed inside an accumulation chamber with a volume of 50 L (±1%). Inside the chamber, a fan is devoted to assuring the homogeneity of thoron concentration. The thoron monitor, RAD7, was calibrated in June 2022 for radon concentration only. Since thoron calibration was not performed, the thoron sensitivity is estimated to be 0.00343 cpm per Bq m^{-3}, which is the half of the radon sensitivity in sniff mode, as reported by the RAD7 manual. A humidity and temperature sensor inside the chamber records data of environmental parameters. The detector has been operated in thoron protocol and the air flow rate of the inner pump set accordingly at around 0.7 L per minute. Thoron measurements are reported by the instrument each 5 minutes. Measurements performed on the samples have had a duration of about 24 h. Data obtained have been managed to obtain the arithmetic mean and the corresponding uncertainty calculated by considering both systematic and stochastic components. The systematic component has been set to 25%, according to Durridge® calibration certificate. The uncertainty of the exhaling surface has been set to 4% and the volume uncertainty of the accumulation volume has been set to 1%. The thoron exhalation rate was calculated using Eq. (1). The homogeneity of thoron concentration inside the chamber has been checked through several measurements performed on highly exhaling material samples by sampling the air inside the chamber at different height from the sample.

2.3 Statistical methods

In recent years, the evaluation of proficiency tests, including those for radon and thoron exhalation measurements (De With et al., 2021; Petropoulos et al. 2001), has traditionally relied on classical statistical methods. However, to more effectively account for potential outliers, robust analysis techniques are now recommended (ISO, 2022). In the present work, the results of the proficiency tests will be evaluated using both classical and robust methods, and the respective assessments will be compared. Descriptions of the methodologies employed are provided below.

2.3.1 Classical analysis

Classical analysis methods for evaluating proficiency tests have typically relied on using the arithmetic mean of all participants' results as a benchmark for comparing individual performances. The standard deviation is generally employed to assess the variability of test scores among participants. However, this type of analysis is often influenced by outliers, which can skew the results. Therefore, robust analysis techniques are specifically developed to minimize the impact of outliers, thereby maintaining the accuracy and reliability of the overall evaluation.

2.3.2 Robust analysis

In accordance with the statistical methods for use in proficiency testing by interlaboratory comparison (ISO, 2022), assigned values and uncertainties are calculated by applying an iterative scheme. This is called the robust analysis and is presented below. The reported and assigned values determine an evaluation of the results on three separate accounts, denoted as accuracy, precision and proficiency testing. The three methods of evaluation are also described here.

The robust analysis that is followed in this derivation is a type of iterated winsorisation and can be found in Annex C.3 of ISO 13528:2022 (ISO, 2022). In order to calculate robust estimates of a data set with reported values X_i (with $i = 1, 2, \dots, p$), and reported uncertainty $U(X_i)$, the robust estimate X^* and robust standard deviation S^* are determined with iterated scale. First, the initial values of X^* and S^* are calculated following equations (2) and (3) [1]:

$$X^* = med(X) = \begin{cases} x_{\left\{\frac{p+1}{2}\right\}},\ p\ odd \\ \left[x_{\left\{\frac{p}{2}\right\}} + x_{\left\{1+\frac{p}{2}\right\}}\right],\ p\ even \end{cases} \tag{2}$$

$$S^* = 1{,}483 \cdot med|X_i - X^*|, \tag{3}$$

where p is the number of lab results, where in this case $p = 9$. The initial value of X^* is the median of the reported values X_i. The initial value for the standard deviation S^* also factors in X^* by taking the median of the difference between each reported value and the initial value of X^*. Since the initial values are based on the median, over each iteration this is only one value. The values of X^* and S^* are updated according to equations (4) to (7) by introducing the δ parameter [1]:

$$\delta = 1{,}5 \cdot S^* \tag{4}$$

The δ parameter is used to change X_1^* to X_9^* depending on the values of X_1 to X_8 respectively.

$$X_i^* = f(x) = \begin{cases} X^* - \delta,\ when\ X_i < X^* - \delta \\ X^* + \delta,\ when\ X_i > X^* + \delta \\ X_i,\ otherwise \end{cases} \tag{5}$$

One ‘new’ robust estimate is then calculated by taking the average of the eight individual estimates.

$$X^* = \sum_{i=1}^{p} \frac{X_i^*}{p} \tag{6}$$

Just as in equation (6), a new value of S^* is calculated according to equation (7):

$$S^* = 1{,}134 \cdot \sqrt{\sum_{i=1}^{p} \frac{(X_i^* - X^*)^2}{p-1}} \tag{7}$$

These new values of the robust estimates are the starting point for the next iteration. By repeating the process outlined in equations (4) to (7), X^* and S^* are expected to converge. After 20 iterations, the robust average and its standard deviation for both the tape and lacquer data have sufficiently converged to meet the same number of significant digits as in the data sets. When the assigned value X_{pt} is derived as a robust average ($X_{pt} \approx X^*$), the standard uncertainty of the assigned value X_{pt} may be estimated as $U(X_{pt})$ in equation (8) below:

$$U(X_{pt}) = 1{,}25 \cdot \frac{S^*}{\sqrt{p}}. \tag{8}$$

2.3.2.1 Accuracy testing

The relative bias R_b between the reported and the assigned value (consensus value from participant results as described in Annex C of the ISO 13528 (ISO, 2022) is expressed by the following equation (9):

$$R_b = \frac{X_i - X_{pt}}{X_{pt}}. \tag{9}$$

The relative bias is compared to the Maximum Acceptable Relative Bias (MARB) which has been determined as 20% by the steering committee, considering the radioanalytical methods, the level of radioactivity, and, the complexity of the analysis. If $|R_b| \leq MARB$, the result will be accepted for accuracy.

2.3.2.2 Precision testing

Based on fit-for-purpose and good laboratory practice principles, the P value is calculated according to equation (10) below:

$$P = \sqrt{\left(\frac{U(X_{pt})}{X_{pt}}\right)^2 + \left(\frac{U(X_i)}{X_i}\right)^2}. \quad (10)$$

The P value is a combination of the assigned and reported uncertainties divided by their respective value. Then, the individual results are squared, summed and the square root is taken to define a method of precision testing. The expanded relative combined uncertainty should cover the relative bias to calculate the P value:

$$|R_b| \leq k \cdot P \,, \quad (11)$$

where k is the coverage factor, for 99% confidential level, $k = 2.58$. If the result is between the ± $MARB$ values, but it is not overlapping the assigned value within the uncertainty, this equation is used to decide if they are significantly different or not. The P value is also compared to the $MARB$. If equation (11) holds, along with equation (12) below:

$$P \leq MARB. \quad (12)$$

the reported results are considered to be acceptable for precision. The result will be assigned unacceptable for precision if either condition is not fulfilled. A final score is assigned according to the detailed evaluation described above, taking into account both accuracy and precision. The possible scores are listed below:

- Accepted: when accuracy and precision are both considered to be acceptable.
- Not Accepted: when the accuracy is considered to be unacceptable
- Warning: when accuracy is considered to be acceptable, but precision is not.

2.3.2.3 Proficiency testing

As additional information, a z score parameter for a proficiency test is determined in equation (13):

$$z = \frac{X_i - X_{pt}}{\sigma_{pt}}, \quad (13)$$

where σ_{pt} is the standard deviation for proficiency assessment, where $\sigma_{pt} \approx U(X_{pt})$. The assumption was made to estimate the standard deviation for proficiency assessment σ_{pt} as the uncertainty of the assigned value $U(X_{pt})$. Normally σ_{pt} depends on information of the repeatability σ_r and reproducibility σ_R of the method, see equation (14):

$$\sigma_{pt} = \sqrt{\sigma_R^2 - \sigma_r^2\left(1 - \frac{1}{m}\right)}, \quad (14)$$

where m is the number of replicate measurements each participant is to perform in a round of the proficiency testing scheme. Since in this case $m = 1$, the standard deviation for proficiency testing is equal to the standard deviation of reproducibility, which has been estimated to be the calculated standard uncertainty.

The conventional interpretation of z scores is as follows (see ISO/IEC 17043:2010, B.4.1):

- A result that gives $|z| \leq 2{,}0$ is considered to be acceptable.
- A result that gives $2{,}0 < |z| < 3{,}0$ is considered to give a warning signal.
- A result that gives $|z| \geq 3{,}0$ is considered to be unacceptable (or action signal).

However, it is important to note that the estimated consensus value (X_{pt}) in this study may contain unknown bias arising from variations in methodologies and operating conditions, which can affect the accuracy of results obtained by individual laboratories - a limitation acknowledged in ISO 13528. In particular, differences in operating humidity conditions across laboratories may have influenced the measurement results, especially for electrostatic-based thoron detectors, as reported by He et al. (2023). Consequently, the z-scores derived in this context may also reflect a certain degree of bias. Therefore, the z-score should not be interpreted as a strict criterion for determining acceptability or unacceptability, but rather as a guiding parameter to support laboratories in refining their methodologies and minimizing potential under- or over-estimations.

3 RESULTS AND DISCUSSION

3.1 Results

For each laboratory, the thoron exhalation rates from both samples are presented in Table 4. From a comparison between classical and robust analysis, it emerges that the arithmetic mean and the robust average for sample I are both 0.39 Bq m^{-2} s^{-1}, while the values for sample II are respectively 0.54 and 0.53 Bq m^{-2} s^{-1}. The robust average values are used as the consensus value (assigned values – X_{pt}) from the results of the participants. The standard deviation calculated using the robust method (S^*) appears to be around 10% higher than the one calculated using the classical method. In addition, the uncertainty $U(X_{pt})$ assigned to the consensus value X_{pt} using the robust methods was around 25% greater than compared to the standard error of the arithmetic mean. This means that the acceptance criteria using the robust analysis are less stringent than those using the classical analysis. A graphical representation of the results, accompanied by a comparison with the assigned values (X_p) and their respective confidence intervals, is presented in Figure 2 for both samples. As shown in Figure 2, for half of the laboratories, the results are within one assigned uncertainty $U(X_{pt})$ for both the samples used in the intercomparison.

Detailed results for accuracy (R_b), precision (P value) and z-score are reported in Table 5. The outcomes of the three evaluation parameters differ substantially. Regarding the *accuracy evaluation*, the relative bias R_b seems to be a balanced measure for intercomparison. For both the samples, the median bias is lower than 10%. This indicates that approximately 50% of the results do not exceed the Maximum Acceptable Relative Bias (MARB), which was set at 20% (section 2.3.2). Moreover, for all the laboratories – with the exception of F1 – results are within the 50% of the assigned values (see Figure 2). A further insight into the measurement repeatability is demonstrated when plotting the relative biases of the two samples for each laboratory (see Figure

3). In general, the repeatability appears to be satisfactory for all laboratories, as evidenced by the points on the *Youden plot* (Figure 3) being relatively close to the bisecting line. This is particularly true for those with the greatest bias, indicating that it is likely that these biases are primarily attributable to systematic uncertainties (or *type B* uncertainty as defined by GUM). These are mainly due to the calibration and affect both the measured samples in a similar manner.

In this context it is also important to mention that some limited measurements were carried out using passive detectors (F2). The thoron exhalation rates were found to be equal to 0.34 and 0.46 Bq m^{-2} s^{-1}, for Sample I and Sample II, respectively. The bias was estimated at approximately -15% for both samples, and with the results still lying on the bisecting line of the *Youden plot* good measurement repeatability was confirmed. The observation that these biases are considerably lower than those observed in the active measurements (exceeding +40% for both samples) provides further support on the role of calibration. The impact of this *type B* uncertainty is well recognized also observing the ratio of the thoron exhalation rates measured for the two samples (see Table 4). Since the same experimental devices are employed in each laboratory, the ratio of thoron exhalation measurements is not influenced by uncertainties associated with the calibration factor. Indeed, the coefficient of variation (CV) of the ratio (20%) is considerably lower than that of the thoron exhalation rate of the sample I (CV = 33%) and sample II (CV = 25%).

Regarding the *precision*, the two criteria resulting in acceptance for the evaluation of precision (section 2.3.3) might be too strict. Especially *P values* were higher than 20% (MARB) – see equation (12) – in most cases. Notably, *P values* range from 19% to 31% (for sample I) and from 15% to 30% (for sample II). However, considering other potential sources of variability (which will be addressed subsequently in the discussion), it is reasonable to assume that a MARB exceeding 20% (for example, equal to 30%-35%) may be deemed acceptable. In this instance, all laboratory values would be acceptably precise.

For the proficiency testing using the *z-score*, the assumption was made to estimate the standard deviation for proficiency assessment σ_{pt} as the uncertainty of the assigned value $U(X_{pt})$. Results are within the accepted range of $|z| \leq 2.0$ for 5 out of 9 of the applied methods. Nevertheless, the above-mentioned assumption of greater variability would increase the uncertainty of the assigned value and consequently reduce the *z-score* values for the same test.

3.2 Discussion

From the literature, the primary factors influencing thoron exhalation measurements are the sampling flow rate (Sorimachi et al., 2016; Tamakuma *et al*, 2021: Hosoda *et al*, 2022) and humidity (Janik *et al.*, 2015; He et al., 2023). The following sections provide a concise analysis of these factors, emphasizing their potential influence on the observed variability in the present study. Additionally, recommendations for improving the results of the future round-robin tests are proposed.

3.2.1 The impact of sampling flow rate on the thoron exhalation measurements

Due to the short half-life of thoron, the sampling flow rate likely affects the responses of the active monitors. In fact, Hosoda et al. (2022) showed that the thoron exhalation rate measured at the commonly used flow rate of 0.7 L min^{-1} – it is the sampling flow rate generally used for the internal sampling pump of the RAD7 – was found to be a factor of 5 to 6 higher when compared with a value of 0 L min^{-1}. Moreover, in a thoron intercomparison for continuous monitor, it was found that the flow rate significantly impacted the response of thoron measurement instruments (Sorimachi et al., 2016), with calibration factors varying from 0.75 to 2.32 depending on the flow rate. This means that monitor’s response can vary by a factor of about 3. Notably, the data obtained from the three laboratories using RAD7 monitors with an identical pump flow rate and the same configuration of the apparatus for sampling, showed a relative standard deviation (k=1) of approximately 20% (Sorimachi et al., 2016). This variability is comparable to that observed in the present study (see Table 4).

For round-robin tests of thoron exhalation in the future, it is recommended to determine the calibration factor for each monitor individually, as experimental results indicate that the calibration factor values depend on the pump flow rate. It is also advisable to conduct periodic calibration of the monitor, along with an assessment of the flow rate during thoron measurements (Sorimachi et al., 2016; Hosoda et al. 2022).

3.2.2 The impact of humidity on the thoron exhalation measurements

An influence of the moisture of the sample on the exhalation has been found in previous studies both for radon and for thoron. In general, very small and very high moisture leads to a decrease of the exhalation rate, in the first case in particular due to a reduced emanation into the pores of the sample and in the second case due to impeded diffusion through the pores to the surface of the sample (Stranden et al., 1984; Hosoda et al., 2007). For soil samples, the decrease at high moisture occurs at moisture values above about 10 or even 20% (Hosoda et al., 2022).

In practice, it might be easier and more reasonable to monitor the humidity of the ambient air around the sample instead of the moisture of the sample, especially in buildings and also in laboratory environments. This was done during the measurements in this study. The relation between ambient humidity and sample moisture depends on the sample material. However, even humidities up to 100% lead to sample moisture of only a few percent, significantly below the range of high moisture and decreased exhalation (Leelamanie, 2010). Therefore, in a study by Meisenberg and Tschiersch (2011) on the influence of ambient humidity, no decrease on the thoron exhalation was found. Since indoor building material is neither subject to precipitation such as rainfall nor typically to very dry conditions, its moisture typically falls in a range of relatively high radon and thoron exhalation. Janik et al. (2015) investigated the thoron exhalation rates from granite and brick samples across a range of absolute humidities (1-24 g m^{-3}). Their findings indicated that, for granite, the thoron exhalation rate approximately doubled within this humidity range. Given the differing experimental conditions of relative humidity and temperature in the current study's laboratories, the absolute humidity range is approximately 7-14 g m^{-3}. According to Janik et al. (2015), within this specific range, a variation in thoron exhalation rate of about 20% could be expected. Therefore, a future round-robin tests on radon and thoron exhalation should define requirements on the humidity at which the samples must be conditioned before the measurements.

Moreover, careful consideration should be given to the humidity conditions within the detector's measurement chamber during both calibration and measurement. Air humidity is a critical factor affecting the sensitivity of thoron activity concentration measurements, particularly for monitors employing electrostatic collection techniques in conjunction with alpha spectrometry analysis. As reported by He et al. (2023), the sensitivity of such detectors to thoron can decrease by a factor of three when absolute humidity increases from 0 to 20 g m^{-3}. Consequently, measurements should either be conducted under humidity conditions consistent with those used during calibration or be appropriately corrected for deviations. Additionally, any uncertainty arising from humidity fluctuations within the measurement chamber should be taken into account.

4 CONCLUSIONS

A unique intercomparison study on the thoron exhalation rate from building materials was performed. Eight laboratories participated in the study using their own methods and procedures for determining the thoron exhalation rate. In the study two samples were tested that were circulated among the participants, the samples were made from phosphogypsum and unfired clay that are available as mainstream building material. Following the measurement of the samples, results were collected and a statistical analysis according to ISO 13528:2022 for proficiency testing was performed.

The assigned value for the exhalation rate of the phosphogypsum and unfired clay was respectively (0.39±0.15) and (0.53±0.15) Bq m^{-2} s^{-1}. Z-scores were below a value of 3 for seven out of the nine methods that were used. The parameters for bias (R_b) and precision (P) are, with the exception of one, within 50%. Details on the type A and B uncertainties were provided by the laboratories, indicating that in most cases the uncertainty in the detector calibration was dominant. For this reason, the ratio in the measured value of sample I and II was obtained enabling a comparison of methods without the uncertainty in the calibration. As a consequence, the variation in results was reduced by approximately 50%. These findings strongly indicate that a key item for improving thoron measurement in future is to provide more robust calibration methods for thoron detection. At present, calibration sources for thoron are poorly available, and the study has reported on a variety of methods that were used by the participants.

To improve consistent measurement of the thoron exhalation rate the development of an harmonised standard would be much welcomed. Such standard should provide guidance on the calibration of the detector. Other aspects that would benefit from harmonisation are: climate conditions during sample preparation and testing, procedures for determination of the exhalation rate and its uncertainty characteristics, and guidance on material aging and spatial variations.

5 REFERENCES

Čeliković, I.T., Pantelić, G.K., Živanović, M.Z., Vukanac, I.S., Krneta Nikolić, J.D., Kandić, A.B, Lončar, B.B. (2020) Radon and thoron exhalation rate measurements from building materials used in Serbia. *Nukleonika*, 65:2, 111-114. https://doi.org/10.2478/nuka-2020-0017.

Chen, J. (2022) Assessment of thoron contribution to indoor radon exposure in Canada. *Radiat. Environ. Biophys.*, 61:161–167. https://doi.org/10.1007/s00411-021-00956-0.

De With, G., De Jong, P. (2011) CFD modelling of thoron and thoron progeny in the indoor environment. *Rad. Prot. Dosim.*, **145**:2–3, 138–144. https://doi.org/10.1093/rpd/ncr056.

De With, G., De Jong, P., Röttger, A. (2014) Measurement of thoron exhalation rates from building materials. *Health Phys.*, **107**:3, 206-212. https://doi.org/10.1097/HP.0000000000000105.

De With, G., De Jong, P. (2016) Impact from indoor air mixing on the thoron progeny concentration and attachment fraction. *J. Environ. Radio.*, **158**, 56-63. https://doi.org/10.1016/j.jenvrad.2016.02.019.

De With, G., Smetsers, R.C.G.M., Slaper, H., De Jong, P. (2018) Thoron exposure in Dutch dwellings – An overview. *J. Environ. Radio.*, **183**, 73-81. https://doi.org/10.1016/j.jenvrad.2017.12.014.

De With, G., Kovacs, T., Csordas, A., Tschiersch, J., Yang, J., Sadler, S.W. Meisenberg, O. (2021) Intercomparison on the measurement of the thoron exhalation rate from building materials. *J. Environ. Radio.*, **228**, 106510. https://doi.org/10.1016/j.jenvrad.2020.106510.

Folkerts, K.H., Keller, G., Muth, H. (1984) Experimental investigations on diffusion and exhalation of ^{222}Rn and ^{220}Rn from building materials. *Rad.. Prot. Dosim.*, 7**(**1-4), 41-44. https://doi.org/10.1093/oxfordjournals.rpd.a082959.

Frutos-Puerto, S., Pinilla-Gil, E., Andrade, E., Reis, M., Madruga, M.J., Rodríguez, C.M. (2020) Radon and thoron exhalation rate, emanation factor and radioactivity risks of building materials of the Iberian Peninsula. *Peer J* **8**, e10331. https://doi.org/10.7717/peerj.10331.

He, C., Wang, H., Zhang, L., Guo, Q. (2023) Impact of humidity and flowrate on the thoron measurement sensitivity of electrostatic radon monitors. *J. Radiol. Prot.* **43**(1), 011504. https://doi.org/10.1088/1361-6498/acb067.

Hosoda, M., Shimo, M., Sugino, M., Furukawa, M., Fukushi, M. (2007) Effect of Soil Moisture Content on Radon and Thoron Exhalation, *J. Nucl. Sci. Technol*, **44**(4), 664-672 https://doi.org/10.1080/18811248.2007.9711855.

Hosoda, M., Yamada, R., Kobyashi, H., Tamakuma, Y., Nugraha, E.D., Hashimoto, H., Negami, R., Kranrod, C., Omori, Y., Tazoe, H., Akata, N., Tokonami, S. (2022) Influence of sampling flow rate on thoron exhalation rate measurements by the circulation method, *Rad. Prot. Dosim.*, **198**(13-15): 904-908. https://doi.org/10.1093/rpd/ncac004.

Hu, J., Wu, Y., Saputra, M.A., Song, Y., Yang, G., Tokonami, S. (2022) Radiation exposure due to ^{222}Rn, ^{220}Rn and their progenies in three metropolises in China and Japan with different air quality levels. *J. Environ. Radio.*, **244-245**, 106830. https://doi.org/10.1016/j.jenvrad.2022.106830.

ISO (2022) Statistical methods for use in proficiency testing by interlaboratory comparison. The International Organization for Standardization, ISO 13528:2022.

Janik, M., Omori, Y., Yonehara, H. (2015) Influence of humidity on radon and thoron exhalation rates from building materials. *Appl. Radiat. Isot.*, **95**, 102-107. https://doi.org/10.1016/j.apradiso.2014.10.007.

Kanse, S., Sahoo, B.K., Sapra, B.K., Mayya, Y.S. (2013) Powder sandwich technique: A novel method for determining the thoron emanation potential of powders bearing high ^{224}Ra content. *Radiat. Meas.*, **48**, 82-87. https://doi.org/10.1016/j.radmeas.2012.10.014.

Kanse, S.D., Sahoo, B.K., Gaware, J.J., Prajith, R. and Sapra, B.K. (2020) A study of thoron exhalation from monazite-rich beach sands of High Background Radiation Areas of Kerala and Odisha, India (**75**, 1465, 2016). *Environ. Earth Sci.*, **79**:3, 72. https://doi.org/10.1007/s12665-020-8810-2.

Keller, G., Folkerts, K.H., Muth, H. (1982) Method for the determination of ^{220}Rn (Radon) and ^{220}Rn (Thoron) –Exhalation rates using alpha- spectroscopy. *Rad. Prot. Dosim.*, **3**(1-2), 83-89. https://doi.org/10.1093/oxfordjournals.rpd.a081158.

Keller, G., Schütz, M. (1996) Results of special ^{220}Rn measurements. *Environ. Int.*, 22, S1135-S1138.

Keller, G., Hoffmann, B., Feigenspan, T. (2001) Radon permeability and radon exhalation of building materials. *Sci. Total. Environ.*, **272**(1-3), 85-89. https://doi.org/10.1016/s0048-9697(01)00669-6.

Kodaira, S., Morishige, K., Kawashima, H., Kitamura, H., Kurano, M., Hasebe, N., Koguchi, Y., Shinozaki, W., Ogura, K. (2016) A performance test of a new high-surface-quality and high-sensitivity CR-39 plastic nuclear track detector – TechnoTrak. *Nucl. Instrum. Methods Phys. Res., B*, **383**, 129–135. https://doi.org/10.1016/j.nimb.2016.07.002.

Leelamanie, D.A.L. (2010) Changes in Soil Water Content with Ambient Relative Humidity in Relation to the Organic Matter and Clay, *Int. J. Trop. Agric. Res. Ext.*, **13**(1), 6-10, https://doi.org/10.4038/tare.v13i1.3130.

Meisenberg, O., Tschiersch J. (2011) Thoron in indoor air: Modeling for a better exposure estimate, *Indoor Air*, **21**(3), 240-52, https://doi.org/10.1111/j.1600-0668.2010.00697.x

Meisenberg, O., Mishra, R., Joshi, M., Gierl, S., Rout, R., Guo, L., Agarwal, T., Kanse, S.M., Irlinger, J., Sapra, B.K., Tschiersch, J. (2017) Radon and thoron inhalation doses in dwellings with earthen architecture: Comparison of measurement methods. *Sci. Total Environ.*, **579**, 1855-1862. https://doi.org/10.1016/j.scitotenv.2016.11.170

NEN (2001) Radioactivity measurements – Determination method of the rate of the radon exhalation of dense building materials. NEN 5699(en). Nederlands Normalisatie-instituut, Delft, the Netherlands.

Nguyên, N.T.A., Nguyên-Thùy, D., Nguyên-Van, H., Nguyên-Hai, N., Schimmelmann A. (2021) Radioactive thoron ^{220}Rn exhalation from unfired mud building material into room air of earthen dwellings. *Front. Earth Sci.*, **9**, 629241. https://doi.org/10.3389/feart.2021.629241.

Petropoulos, N. P., Anagnostakis, M. J., & Simopoulos, S. E. (2001) Building materials radon exhalation rate: ERRICCA intercomparison exercise results. *Sci. Total Environ.*, **272**(1-3), 109-118. https://doi.org/10.1016/S0048-9697(01)00674-X.

Pornnumpa, C., Oyama, Y., Iwaoka, K., Hosoda, M., Tokonami, S. (2018) Development of Radon and Thoron Exposure Systems at Hirosaki University, *Radiat. Env. and Med.*, 7(1), 13-20. https://doi.org/10.51083/radiatenvironmed.7.1_13.

Porstendörfer, J. (1994) Properties and behaviour of radon and thoron and their decay products in the air. *J. Aerosol Sci.*, **25**(2), 219-263. https://doi.org/10.1016/0021-8502(94)90077-9.

Röttger, A., Honig, A., Dersch, R., Ott, O., Arnold, D. (2010) Primary standard for the activity concentration of ^{220}Rn (thoron) in air. *Appl. Radiat. Isot.*, **68**, 1292–1296. https://doi.org/10.1016/j.apradiso.2010.01.004.

Sahoo, B.K., Sapra, B.K., Kanse, S.D., Gaware, J.J., Mayya, Y.S. (2013) A new pin-hole discriminated ^{222}Rn/^{220}Rn passive measurement device with single entry face. *Radiat. Meas.*, **58**, 52-60. https://doi.org/10.1016/j.radmeas.2013.08.003.

Sanada, T. (2021) Measurement of Indoor Thoron Gas Concentrations Using a Radon-Thoron Discriminative Passive Type Monitor: Nationwide Survey in Japan. *Int. J. Environ. Res. Public Health*, 18, 1299. https://doi.org/10.3390/ijerph18031299.

Shang, B., Tschiersch, J., Cui, H., Xia, Y. (2008) Radon survey in dwellings of Gansu, China: the influence of thoron and an attempt for correction. *Radiat. Environ. Biophys*. 47, 367-373. https://doi.org/10.1007/s00411-008-0163-2.

Smetsers, R.C.G.M., Blaauboer, R.O., Dekkers, F., Slaper, H. (2018) Radon and thoron progeny in Dutch dwellings. *Radiat. Prot. Dosimetry*, **181**(1), 11–14. https://doi.org/10.1093/rpd/ncy093.

Sorimachi, A., Janik, M., Tokonami, S., Ishikawa, T. (2016) An intercomparison done at NIRS, Japan on continuous monitors for measuring 220Rn concentration. *Appl. Radiat. Isot.,* **107**, 145-151. https://doi.org/10.1016/j.apradiso.2015.10.007.

Sreenath Reddy, M., Yadagiri Reddy, P., Rama Reddy, K., Eappen, K.P., Ramachandran, T.V., Mayya, Y.S. (2004) Thoron levels in the dwellings of Hyderabad city, Andhra Pradesh, India. *J. Environ. Radioact.,* **73**, 21–28. https://doi.org/10.1016/j.jenvrad.2003.07.002.

Stranden, E., Kolstad, A. K., Lind, B. (1984) The Influence of Moisture and Temperature on Radon Exhalation. *Radiat. Prot. Dosimetry*, **7**(1-4), 55–58. https://doi.org/10.1093/oxfordjournals.rpd.a082962.

Tamakuma, Y., Kranrod, C., Jin, Y., Kobayashi, H., Nugraha, E. D., Sanpei, A., ... & Tokonami, S. (2021) Characterization of commercially available active-type radon–thoron monitors at different sampling flow rates. *Atmosphere*, **12**(8), 971. https://doi.org/10.3390/atmos12080971

Tokonami, S., Takahashi, H., Kobayashi, Y. Zhuo, W., Hulber, E. (2005) Up-to-date radon-thoron discriminative detector for a large scale survey. *Rev. Sci. Instrum.*, **76**, 113505. https://doi.org/10.1063/1.2132270.

Tschiersch, J. and Meisenberg, O. (2008) Thoron exhalation from building material and related indoor concentrations. In: Strand, P., Brown, J., Jølle, T. (Eds.) The International Conference on Radioecology & Environmental Radioactivity. Bergen, Norway, 15-20 June 2008, Part 1 (ISBN 978-82-90362-25-1) 415-418.

Tuccimei, P., Moroni, M., Norcia, D. (2006) Simultaneous determination of ^{222}Rn and ^{220}Rn exhalation rates from building materials used in Central Italy with accumulation chambers and a continuous solid state alpha detector: influence of particle size, humidity and precursors concentration. *Appl. Radiat. Isot.,* **64**, 254–263. https://doi.org/10.1016/j.apradiso.2005.07.016.

UNSCEAR (2006) Sources-to-effects Assessment for Radon in Homes and Workplaces, ANNEX E of Effects of Ionizing Radiation, vol. I. United Nations Scientific Committee on the effects of Atomic Radiation. New York.

UNSCEAR (2016) Sources, effects and risks of ionizing radiation, report to the General Assembly. United Nations Scientific Committee on the Effects of Atomic Radiation. New York.

Wang, Z.Y., Lubin, J.H., Wang, L.D., Conrath, S., Zhang, S.Z., Kleinerman, R., Shang, B., Gao, S.X., Gao, P.Y., Lei, S.W., Boice Jr., J.D. (1996) Radon measurement in underground dwellings from two prefectures in China. *Health Phys.,* **70**, 192–198. https://doi.org/10.1097/00004032-199602000-00006.

Yasuda, N., Yamamoto, M., Amemiya, K., Takahashi, H., Kyan, A., Oura, K. (1999) Track sensitivity and the surface roughness measurements of CR-39 with atomic force microscope. *Radiat. Meas.*, **31**, 203-208. https://doi.org/10.1016/S1350-4487(99)00089-X.

TABLES

Table 1 ^{220}Rn exhalation rate for some mainstream building materials as reported in literature.

	Keller and Schütz (1996)	Keller et al. (2001)	De With et al. (2014)	Čeliković et al. (2020)	Frutos-Puerto et al. (2020)
	(Bq m^{-2} s^{-1})	(Bq m^{-2} s^{-1})	(Bq m^{-2} s^{-1})	(Bq m^{-2} s^{-1})	(Bq m^{-2} s^{-1})
Brick	0.01	0.01	0.08	0.04 (0.03-0.06)	
Concrete	0.04 (0.01-0.11)	0.02	0.05 (0.01-0.08)	0.07 (0.03-0.11)	0.01 (0.007-0.02)
Aerated concrete	0.02 (0.01-0.04)	0.02			
Natural gypsum	0.12 (0.01-0.28)	0.01	0.01		0.005 (0.004-0.006)
Phosph. gypsum		0.02	0.42 (0.40-0.42)		

Table 2 Specific activities of the raw materials of the brick sample with tape RV (Sample I) and the brick with lacquer (Sample II) in Bq·kg^{-1}.

	Sample I	Sample II		
		base plaster	kaolinite	sand
C_{Th-232}	51 ± 2	12.4 ± 0.8	107 ± 8	6.5 ± 0.6
C_{Ra-226}	33 ± 1	11.9 ± 0.8	140 ± 11	7.0 ± 1.1

Table 3 Test methods and conditions.

	Chamber ventilation	Chamber* geometry	Ventilation rate	Test conditions	Thoron monitor
Lab A	Ventilated loop	0.3×0.3×0.15 m	300 mL·min^{-1}	20°C, 50%	RAD7
Lab B	Closed loop	0.11×0.11×0.08 m	-	20°C, 50%	RAD7
Lab C	Closed loop	Ø 0.11 m, h 0.05m	-	20°C, 45%	ERS-2-S
Lab D	Closed loop	0.003 m^3	-	20°C, <15%	RAD7
Lab E	Closed loop	0.06×0.22×0.22 m	-	25°C, 7%	RAD7
Lab F1	Closed loop	0.1×0.26×0.26 m	-	18-20 °C, 40-43%	RTM2200
Lab F2	Closed loop	0.1×0.26×0.26 m	-	22-23 °C, 56-59%	CR-39
Lab G	Closed loop	0.15×0.12×0.066 m	-	25°C, 60%	SMART RnDuo
Lab H	Closed loop	Ø 0.45 m, h 0.31 m	-	25°C, 55-65%.	RAD7

* This is the space available for a test sample.

Table 4 Results of the thoron exhalation rates (E_{Tn}). For both samples, the best value (X) with uncertainty $U(X)$ with a coverage factor k =1 is reported for each laboratory. The experimental results are compared using both classical and robust analysis methods.

		Thoron exhalation rates (Bq m^{-2} s^{-1})		**Ratio I/II**
		Sample I	**Sample II**	
	Lab A	0.33 ± 0.05	0.56 ±0.08	1.7
	Lab B	0.35 ± 0.06	0.42 ±0.06	1.2
	Lab C	0.21 ± 0.03	0.39 ±0.04	1.9
	Lab D	0.46 ± 0.12	0.51 ±0.15	1.1
	Lab E	0.26 ± 0.06	0.49 ±0.08	1.9
	Lab F1	0.59 ± 0.10	0.78 ±0.12	1.3
	Lab F2	0.34 ± 0.07	0.48 ±0.11	1.4
	Lab G	0.57 ± 0.06	0.74 ±0.08	1.3
	Lab H	0.39 ± 0.06	0.48 ±0.07	1.2
Classical analysis	*Arithmetic mean (AM)*	**0.39**	**0.54**	**1.4**
	Std deviation (SD)	**0.13**	**0.14**	**0.3**
	CV (SD/AM) (%)	**33**	**25**	**20**
	Std error (SE)	**0.04**	**0.05**	**0.1**
	SE (%)	**11**	**8**	**7**
Robust analysis	*X^* (robust average)*	**0.39**	**0.53**	
	S^* (robust std dev)	**0.15**	**0.15**	
	CV (S^*/X^*) (%)	**38**	**28**	
	$U(X_{pt})$	**0.06**	**0.06**	
	$U(X_{pt})$ (%)	**16**	**11**	

Table 5 Final results for interlaboratory comparison utilizing three statistical methods.

Lab code	**R_b (%)**	**P value (%)**	**Z-score**	**Tested material**
A	-16	22	1.0	Brick with tape RV (Sample I)
B	-10	24	0.7	
C	-46	22	2.9	
D	19	31	1.2	
E	-33	27	2.1	
F1	51	23	3.2	
F2	-13	26	0.8	
G	47	19	3.0	
H	0	22	0.0	
A	4	18	0.3	Brick with lacquer (Sample II)
B	-21	19	1.8	
C	-26	15	2.3	
D	-4	30	0.3	
E	-8	20	0.7	
F1	46	20	4.0	
F2	-14	27	1.3	
G	39	15	3.4	
H	-10	18	0.9	

FIGURES

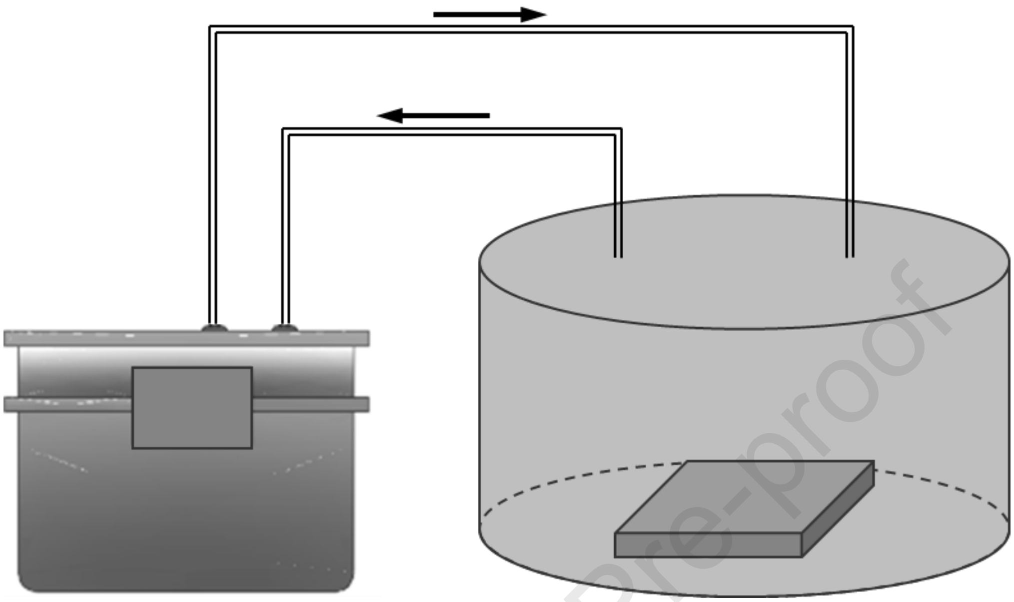

Figure 1 Schematic diagram for the measurement of thoron exhalation from building material as typically used by the participants.

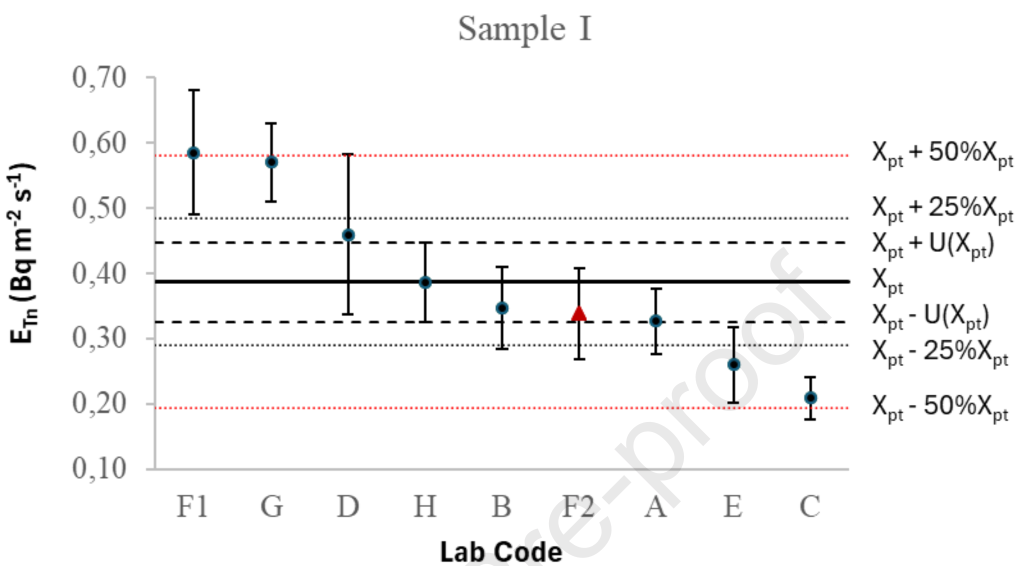

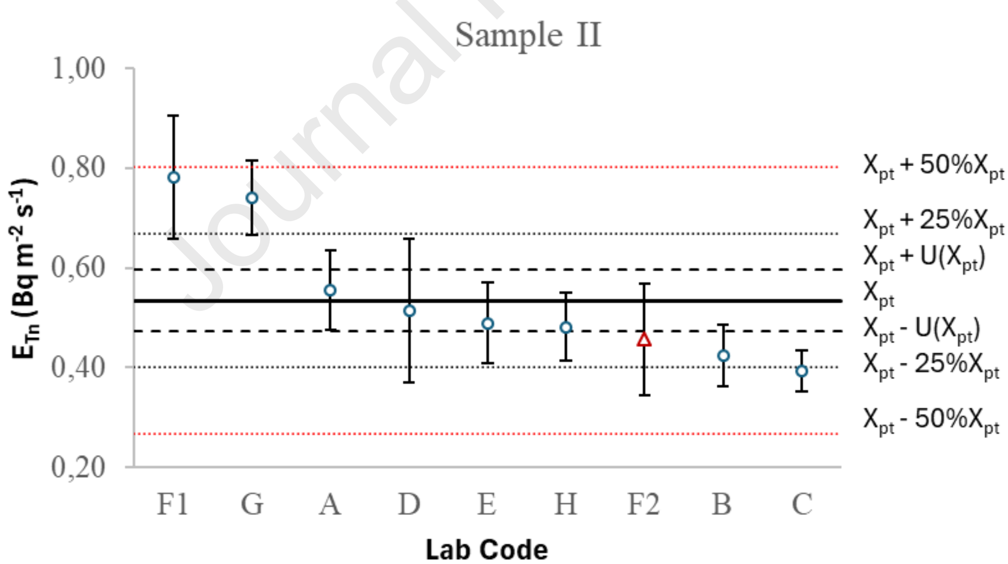

Figure 2 Results of each laboratory (with k=1 uncertainties) for sample I (top) and sample II (bottom) for the active method ○ (circle) and the passive method Δ (triangle). The robust average considered as the assigned value (X_{pt}) is also reported (as solid line) along with its assigned uncertainties U(X_{pt}) with coverage factor k=1. The range of variability of 25% and 50% for the assigned value (X_{pt}) was also reported in the graph.

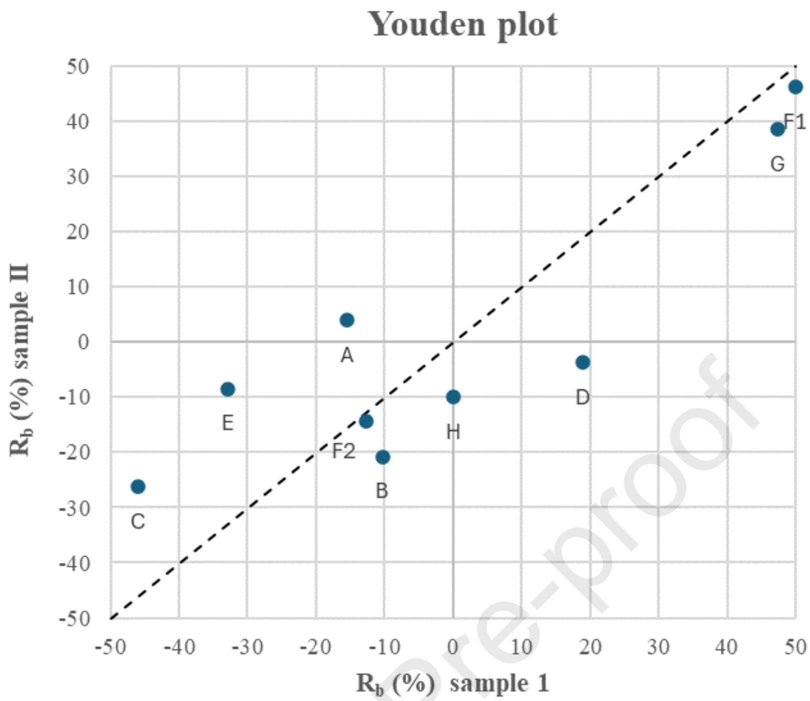

Figure 3 Comparison of the relative bias R_b (%) of two measurements (Youden plot). The labels in the graph indicate the laboratory code.

HIGHLIGHTS

- Intercomparison on thoron exhalation rate from building materials.
- Variations in the measured thoron exhalation rate were up to 50%.
- Development of a robust method for thoron calibration is recommended.

Declaration of interests

☒ The authors declare that they have no known competing financial interests or personal relationships that could have appeared to influence the work reported in this paper.

☐The authors declare the following financial interests/personal relationships which may be considered as potential competing interests: